IEEE Access
Multidisciplinary | Rapid Review | Open Access Journal

Received 21 October 2022, accepted 31 October 2022, date of publication 3 November 2022, date of current version 8 November 2022.

Digital Object Identifier 10.1109/ACCESS.2022.3219065

RESEARCH ARTICLE

Reflection-Type Phase Shifter Integrated With Tunable Power Attenuation Mechanism for Sub-6 GHz Wireless Applications

CHIA-HUNG CHANG[1], (Member, IEEE), JO-YU CHEN[1], CHE-TIEN SHEN[1], MENG-JU TSAI[1], AND TSE-SHENG TAI[2]

[1]Department of Electrical Engineering, National Yunlin University of Science and Technology, Douliou 64002, Taiwan
[2]Department of Electrical Engineering, Feng Chia University, Taichung 40724, Taiwan

Corresponding author: Chia-Hung Chang (changchc@yuntech.edu.tw)

This work was supported by the Ministry of Science and Technology, Taiwan, under Grant MOST 109-2221-E-224-056-MY2 and Grant MOST 111-2221-E-224-011.

ABSTRACT An integrated configuration of the reflection-type phase shifter (RTPS) and attenuator with simultaneous phase and amplitude control is presented for a phased-array front-end beamforming. The phase shift function of the RTPS adopts a quadrature coupler with high/low pass lumped elements and the corresponding π-type C–L–C loads. An RF tuner is subsequently incorporated into the 90° coupler to provide an energy reduction path and applied at the intermediate inductor of the coupler, thereby enabling a tunable transmission power. The merged coupler/RF-tuner realizes a matched and symmetrical structure with less impact on the load impedance variation, which can be regarded as part of the RTPS that performs RF signal degradation and maintains phase shift tuning. Furthermore, the π-type attenuator is incorporated into the RTPS to obtain an adequate power control range for the side-lobe suppression of the beamforming network. The simulated and measured results demonstrate the feasibility and suitability of the network for the proposed merged configuration applied to the phased-array system.

INDEX TERMS Beamforming, phase-array antenna, phase shifter, power control, reflection type, sub-6 GHz.

I. INTRODUCTION

The tendency toward high data rate and high system capacity for the fifth generation (5G) of wireless communication has been developed for massive multiple-input and multiple-output (MIMO) applications [1], [2], [3]. The phase-array beamforming technique plays an important role to concentrate the main beam, which enhances the effective isotropic radiated power (EIRP) and alleviates the propagation loss of the transceiver in particular at RF frequency. Moreover, the phase-array antenna with capabilities of high directivity and steering beams improves the system signal-to-noise ratio (SNR) and spatial diversity. Fig. 1 illustrates an architecture of the phased-array transmitter. Phase-shift and amplitude- tuning circuits are key components to achieve beamforming and calibrate the antenna radiation characteristics, such as beam-offset angle and side-lobe suppression by using genetic algorithm (GA) and least squares error (LSE) techniques [4]. Considering the system plan of a transmitter, the gain control mechanism is commonly realized in the RF band because the carrier leakage and out-band interferers are difficult to synchronously scale down with the transmitted signal as gain variation in the baseband [5], [6]. The RF variable gain amplifier (VGA) is a good candidate to reduce the output power. However, the uncertainties of parasitic effect and propagation loss in the RF transmission path cause power control inaccuracy. Furthermore, a high-power power amplifier (PA) and an absence of well-defined antenna impedance raise power control uncertainty, particularly at the fine-tuning requirement of a phase-array system, which might

The associate editor coordinating the review of this manuscript and approving it for publication was Debdeep Sarkar.

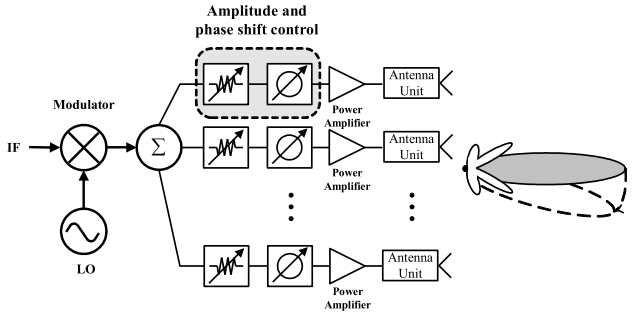

FIGURE 1. Architecture of the phased-array transmitter for RF beamforming.

affect the beamforming efficiency. Moreover, active RF VGA consumes extra DC power and increases circuit complexity. In contrast with an active gain-tuning device, the passive attenuator is an alternative way of focusing on power control with high accuracy and easy implementation. Meanwhile, the lossy RF path can be compensated by the driving amplifier or PA in the transmitter. Considering the phase-array application, the beamforming technique of concentrating on the main beam energy substantially mitigates the propagation loss by the increased EIRP.

From the viewpoint of phase shift, the several reported types of RF-path phase shifter include loaded-line [7], reflection-type [8], switched-type [9], and vector-modulator [10] topologies. The RTPS allows a continuous phase variation with the characteristics of high linearity, bi-directional operation, and zero power consumption compared with the other types of phase shifters [8], [11], [12], [13]. The primary aims for the RTPS design are to increase the phase tuning range and reduce the insertion loss. The conventional RTPS adopts a quadrature 3 dB coupler with reflective loads at through and coupled ports. Varactors with a voltage bias control are used to vary load reactance, which in turn contributes a phase shift at the output terminal. The deviation of insertion losses across the phase tuning range is a concern of the RTPS design. Although a shunt resistor has been reported to reduce transmission loss variation as the varied phase shift, a large insertion loss still occurs at a desired RF frequency [14], [15]. Meanwhile, phase shift is another factor for achieving a tuning phase range of 360°, which is determined by the reflective loads. A varactor-based series/parallel LC resonated load with a single control voltage is proposed to change the load impedance with a phase shift of less than 180° for the case of the maximum to minimum capacitance ratio of less than three [16]. Multiple varactors applied on an asymmetrical C–L–C π-network are further utilized to achieve full a 360° relative phase shift range [17]. However, several control voltages are essential and increase the load design complexity. In a phase-array application, a complicated analog/digital control system is also required to each RTPS. In addition, a transformer-based coupling topology is presented and incorporated into the coupler or reflective loads to obtain a compact design or extend phase shift range, respectively [17], [18], [19]. In [15], [20], the extension of the operating bandwidth with an improved load structure is also proposed in the RTPS design. Nevertheless, most state-of-the-art approaches concentrated on increasing the phase shift range, reducing the transmission loss or bandwidth extension provided by the RTPS design.

In this paper, a new topology is first proposed to integrate the RTPS and the RF tuner with a fine-tunning attenuation for simultaneously performing phase/amplitude control. Instead of separating phase shift and power control circuits, the proposed approach provides a way to merge a coupler/RF-tuner with the reflective loads for the RTPS operation. The design challenge of this hybrid configuration is to realize an RF signal reduction path with less impact on the overall phase deviation and input return loss, which is determined by the reflective load impedance. Accordingly, the concept and feasibility of performing phase and amplitude tuning on the same RTPS circuit are analyzed and investigated in this study. Subsequently, to further investigate the concept of the beamforming behavior in a phased-array antenna system, a 1×8 antenna array integrated with the RTPS is employed to analyze the antenna characteristics of gain pattern and radiated distribution. Therefore, a π-type attenuator for coarse-tuning is also incorporated into the RTPS design to increase the transmitted power dynamic range, which can be also replaced by a variable gain amplifier for coarse tuning.

Section II describes the basic RTPS circuit and the proposed hybrid configuration with power/phase control. Section III depicts the RF tuner integrated with a lumped-element quadrature coupler and π-type attenuator for transmission power with a linear-in-dB control. The merged coupler/RF-tuner is designed to observe the impact of power-tuning on the overall insertion loss and phase shift. Section IV reports the experimental results for the RTPS with a power control mechanism. The beamforming performance of a 1×8 phased-array antenna with the proposed RTPS is also presented. Finally, Section V concludes this work.

II. RTPS PRINCIPLE OF THE OPERATION AND THE PROPOSED RTPS CONFIGURATION

The conventional RTPS configuration is shown in Fig. 2(a), which comprises a branch-line 3-dB coupler and two tunable reflective loads. The quadrature coupler commonly implemented in the distributed transmission line provides equal splitting power with 0° and 90° phase shifts at the through and coupled ports, respectively. The reflected signal is then combined at the output port with a phase shift of Φ, insertion loss of S_{21}, and phase shift range of $\Delta\varphi$, which are derived as follows:

$$\Phi = \angle |S_{21}| = -90 + \angle \Gamma_L, \tag{1}$$

$$|S_{21}|_{dB} = -20 \log |\Gamma_L|, \tag{2}$$

$$\Delta\varphi = \angle \Gamma_L|_{\max} - \angle \Gamma_L|_{\min}, \tag{3}$$

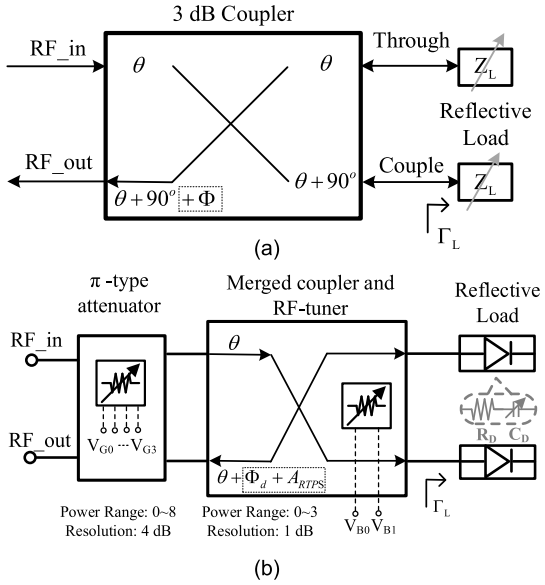

FIGURE 2. (a) Operational principle of conventional RTPS with a 3-dB coupler and (b) merged topology of the coupler/RF-tuner.

where Γ_L is the reflection coefficient at the reflective loads. The total phase shift range is determined by tunning the loaded termination impedance, which can be realized by the varactor to alter effective Γ_L. Thus, low insertion loss and maximized phase shift range are the design parameters for the basic RTPS operation.

Herein, our objective is to investigate the feasibility of the merged RTPS and attenuator with the ability to simultaneously adjust the phase shift and signal amplitude. Fig. 2(b) presents the proposed RTPS topology with a merged coupler/RF-tuner, which allows transmission power control with a fine-tuning of 1-dB step. The RF-tuner is incorporated into the intrinsic hybrid coupler, implemented in an integrated lumped element, to perform power attenuation without affecting the RTPS operation. Accordingly, a tunable amplitude of the RF signal is achieved by the 2-bit binary attenuation control with a power-tuning range from 0 dB to 3 dB, in addition to the original phase shift between the input and output ports, contributed from varying the reflection coefficient of the reflective loads. Suppose that the varactor load is modeled as a varied capacitor C_D and a series parasitic resistor R_D, the equivalent load impedance $Z_L = R_D + jX_C$, where $X_C = {}^{1}\!/\!_{\omega C_D}$, and the corresponding reflection coefficient Γ_L is given by:

$$\Gamma_L = \frac{R_D^2 - Z_o^2 + \left(\frac{1}{\omega C_D}\right)^2 - j\frac{2Z_o}{\omega C_D}}{(R_D + Z_o)^2 + \left(\frac{1}{\omega C_D}\right)^2}, \tag{4}$$

where Z_o is the characteristic impedance. Considering the RTPS operation including merged coupler/RF-tuner and reflective load, the total phase shift Φ_d and insertion loss (IL) can be further derived as follows:

$$\Phi_d = -90^\circ + \tan^{-1}\left(\frac{\frac{2Z_o}{\omega C_D}}{R_D^2 - Z_o^2 + \left(\frac{1}{\omega C_D}\right)^2}\right), \tag{5}$$

$$\begin{aligned} IL &= |S_{21}|_{dB} + A_{\mathrm{RTP}s} \\ &= -20\log\left|\frac{R_D^2 - Z_o^2 + \left(\frac{1}{\omega C_D}\right)^2 - j\frac{2Z_o}{\omega C_D}}{R_D^2 + Z_o^2 + \left({}^{1}\!/\!_{\omega C_D}\right)^2 + 2R_D Z_o}\right| \\ &\quad + (1+\alpha)\,A_{tuner}, \end{aligned} \tag{6}$$

where A_{RTPS} is the equivalent attenuated magnitude of the RTPS, contributed from the RF tuner; A_{tuner} is an ideal 1-dB control attenuation; and α and ω are an interaction factor of the load impedance and operating frequency of the circuit, respectively. According to (5) and (6), the performance of RTPS is determined by the varactor series parasitic R_D, which inevitably depends on the device process and limits the phase variation particularly. The variable C_D can be achieved by tuning the control voltage across a varactor. This study aims to lower the interaction factor of α to accurately control the power attenuation. Thus, the RF-tuner influences the load impedance and contributes to total attenuation value, which will be investigated and analyzed to provide an insight into the design of RTPS with a power control mechanism. From the viewpoint of beamforming application, the π-type network is employed to realize a power-tuning range of 8 dB in a 4 dB step by digital control bits with two attenuation states for coarse tuning. Consequently, the entire hybrid configuration provides a power control range of 11 dB with a resolution of 1 dB.

III. CIRCUIT DESIGN

A. INVESTIGATION OF THE HYBRID LUMPED-ELEMENT COUPLER AND RF TUNER

Considering the 3-dB coupler design, the conventional single-box branch-line coupler requires a quarter wavelength of the transmission line on each side, which occupies a fairly large chip area for the sub-6GHz application. Accordingly, the required 3-dB coupler for RTPS is adopted and realized by using lumped elements, which greatly benefits the system integration and compact circuit at a desired frequency of 3.5 GHz. Fig. 3 presents two types of quadrature coupler in the lumped element means. The conventional coupler with two inductors exhibits a narrow bandwidth, which in turn easily suffers from process variation, as shown in Fig. 3(a). The first-type coupler also has difficulty integrating with the attenuator due to the RF signal loss mainly along the RF transmission path. Consequently, the three-inductor based coupler with high/low pass topology is adopted in this work to integrate with the attenuator to overcome this issue, as shown in Fig. 3(b). The corresponding nominal values of the inductors and capacitors based on the operating frequency, f, can

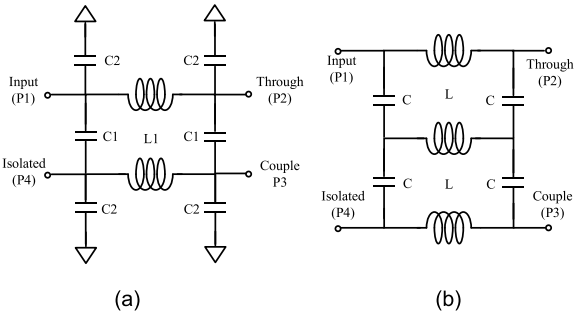

FIGURE 3. (a) Conventional lumped-element quadrature coupler and (b) quadrature hybrid with high/low pass lumped elements.

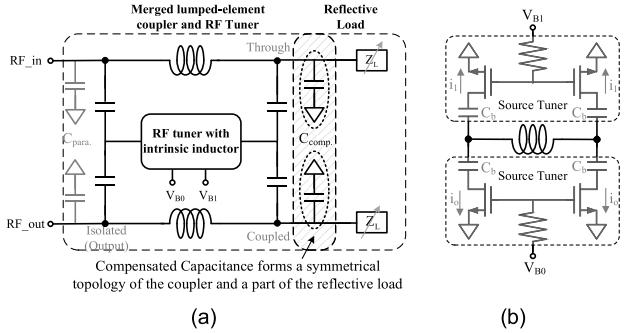

FIGURE 4. (a) Hybrid configuration of the RTPS and RF-tuner using 3-inductor lumped coupler. (b) Schematic of RF tuner.

be calculated as follows [21]:

$$C = \frac{1}{Z_o \cdot 2\pi f}\text{pF}, \tag{7}$$

$$L = \frac{Z_o}{2\pi f}\text{nH}, \tag{8}$$

The RF-path signal can be imposed at two terminals of the intermediate inductor as a symmetrical and a well-matched structure between the input/output transmission paths to perform RF signal source degradation. Fig. 4(a) depicts a hybrid configuration of the RTPS and RF-tuner based on the three-inductor lumped coupler. The RF tuner integrated with the intrinsic inductor of the coupler is utilized to adjust the signal amplitude, as shown in Fig. 4(b). The RF currents (i_o and i_1) flow into the source tuner at the common-mode nodes of the coupler by controlling the supply voltages of V_{B0} and V_{B1} for tuning signal amplitude, thereby enabling RF energy reduction and simultaneously maintaining the RTPS operation. The DC block capacitors (C_b) are used to prevent the DC signal from transistor. Suppose that the MOS-varactor is used as the reflective loads, the merged topology is simulated to analyze the design of the RF tuner. Fig. 5 illustrates the input reflection and transmission coefficients of this proposed topology with respect to the control voltage (V_{B0}) at a desired frequency of 3.5 GHz, while V_{B1} is set to zero to concentrate on one RF-tuner effect. In addition, a fixed W/L ratio of 1.5 μm/0.18 μm changes with transistor fingers to observe the influence of the RF tuner on RTPS performance. It is noted that the transmission power of S_{21} can be indeed attenuated as the increased V_{B0}. A larger transistor size causes a

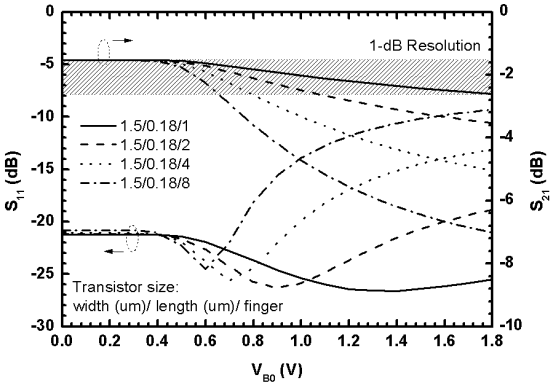

FIGURE 5. Simulated input reflection and transmission coefficients with respect to the control voltage of the RF tuner.

higher degradation due to the increasing i_o. The S_{11} lower than -10 dB is also achieved at all supply voltage states. However, the deviation of S_{11} is gradually growing for large physical transistor sizes in particular at high-voltage states, indicating that the increasing i_o flows into the tuner and contributes to the equivalent input impedance. Notably, the proposed tuner influences the original impedance characteristic of the matching network for the RTPS design, which is relieved by a small transistor size. Additionally, the relative phase deviation of the RTPS in terms of V_{B0} is shown in Fig. 6. The phase shift contribution of the source tuner is also determined by the transistor size. The phase deviation only within 1° can be obtained on a limited transistor fingers of lower than 2. In an ideal RTPS operation with power control mechanism, the S_{11} and phase shift are not supposed to be affected by the RF tuner as the varied S_{21}, which might result in an increased interaction factor α. Consequently, the merged lumped-element coupler/RF-tuner with a fine-tuning of 1 dB resolution is adopted in this work and realized by using digital on/off (0 and 1.8 V) switch control to meet the requirement of linear-in-dB power variation as the system plan. Meanwhile, two RF source tuners are implemented in 2-bit binary-weighted transistor sizes to reduce unwanted deviation of return loss and relative phase variation for achieving a power dynamic range from 0 dB to 3 dB with a 1 dB step. It is worth noting that $C_{para.}$ is the load parasitic capacitance of the π-type attenuator in front of the RTPS, which is absorbed in the quadrature coupler design. In addition, the compensated capacitors $C_{comp.}$ are added to right side of the coupler to form a symmetrical structure of the coupler at resonant frequency. The $C_{comp.}$ can be also regarded as the part of reflective loads, which adopts the π-type C–L–C structure. Therefore, a fixed shunt compensated $C_{comp.}$, series inductor, and parallel variable capacitor form a π-type resonator to vary reflective loads.

B. PROPOSED RTPS DESIGN WITH POWER/PHASE CONTROL MECHANISM

Considering the transmission power control mechanism for the phased-array system, a programmable gain amplifier or

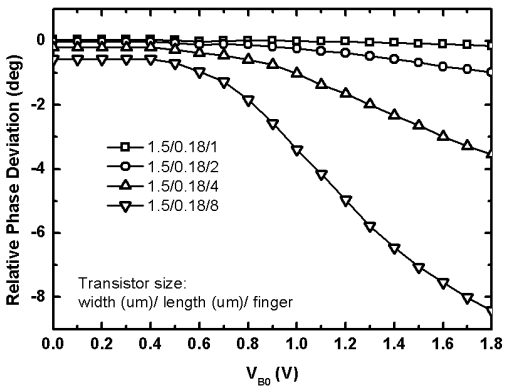

FIGURE 6. Simulated relative phase deviation with respect to the control voltage of the RF tuner.

attenuator is commonly used for power level adjustment. A reciprocal topology of the π-type attenuator with MOSFET switches is adopted in this work for controlling the transmitting power with characteristics of high linearity, power efficiency, and low complexity. Fig. 7(a) shows a π-type attenuator with a coarse-tuning resolution of 4 dB. The voltage-controlled switches (V_{G1} and V_{G1B}) are designed as a complementary operation and applied on transistors M_1 and M_{2a}, M_{2b}, respectively. The equivalent circuit model for the transmission state is depicted in Fig. 7(b) without signal attenuation because $M_{2a,b}$ are off. The input impedance, Z_{in}, has turned into $Z_{in} = R_{on1} \parallel R_s$, where R_{on1} represents a turn-on resistor of M_1, which can be further expressed as follows:

$$R_{on1} = \frac{1}{\mu_n C_{ox} \frac{W}{L} (V_{GS} - V_{TH})}, \tag{9}$$

where μ_n and C_{ox} are the process parameters, V_{GS} is gate voltage with "high" state and V_{TH} is the fixed threshold voltage of around 0.6 V. It is revealed that R_{on1} is in terms of the physical size (W/L) of the transistor. Consequently, a larger transistor size is supposed to be determined to reduce the transmission resistance and then minimize insertion loss. However, a large switch size raises a concern of parasitic capacitance. Herein, the undesired output parasitic capacitances are incorporated and neutralized in the subsequent lumped-element coupler at resonant frequency. By contrast, Fig. 7(c) illustrates the equivalent circuit at the attenuation state. Suppose that the input/output impedance are perfectly

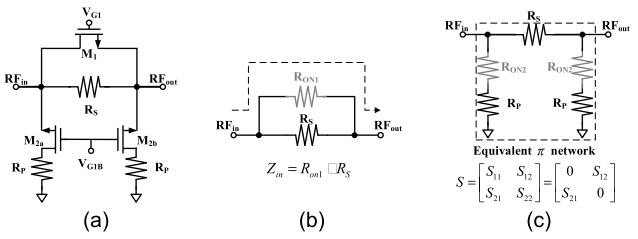

FIGURE 7. (a) π-type attenuator, and the corresponding equivalent circuit model with (b) signal transmission and (c) signal degradation.

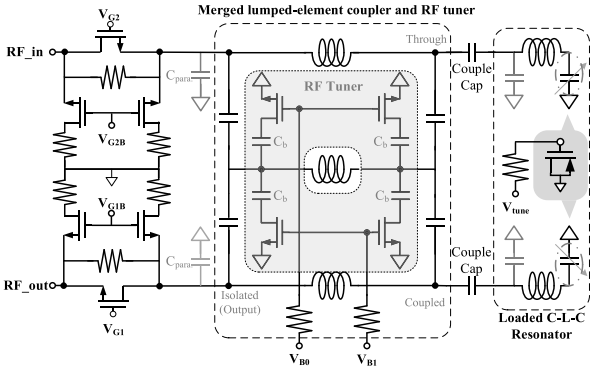

FIGURE 8. Topology of the proposed RTPS with power control mechanism.

matched, the series/shunt resistors (R_S and R_P) can be further expressed as:

$$R_S = 50\left(\frac{1 - S_{21}^2}{2S_{21}}\right), \tag{10}$$

$$R_P = 50\left(\frac{1 + S_{21}}{1 - S_{21}}\right) - R_{on2}, \tag{11}$$

where S_{21} is the transmission coefficient of the π-type attenuator. The R_S and R_P are thus determined by a given attenuation value. Fig. 8 shows the topology of the proposed RTPS with power control mechanism, which comprises π-type attenuation stages, a merged coupler/RF-tuner, and reflective loads. The π-type attenuators can adjust the power transmission level with a dynamic range of 8 dB in a 4-dB step. The effective capacitive loadings due to a large transistor size are regarded as part of the hybrid 3-dB coupler design, which is implemented in a three-inductor lumped element for facilitating further integration with the fine-tuning attenuation. The merged couple/RF-tuner not only provides digital-assisted attenuation with 2-bit binary array control but also performs a phase shift at through/coupled ports for the RTPS operation. Accordingly, the configuration of a loaded C–L–C resonator is adopted as the reflection loads. The transistor-based MOS-varactors are utilized as a substitute for the one-sided capacitive loads. Although a complex topology with an asymmetrical C-L-C π-network can be used to extend the phase shift range, the number of varactors and independently controlled voltages are increased. Consequently, the RTPS design is primary concerned with the attenuation behavior of the merged coupler/RF-tuner. A varactor with a single supply voltage of V_{tune} is only applied on the terminated side of the MOS varactor for phase shifting. A constant compensated capacitor is added to the left side of the loaded resonator.

IV. MEASUREMENT RESULTS

The reflection-type phase shifter integrated tunable transmission power mechanism was implemented in the TSMC 0.18 μm CMOS technology. The die photograph for the test chip is displayed in Fig. 9. The chip occupies 1.18 mm $\times$ 1.06 mm of the die area, including the I/O pads.

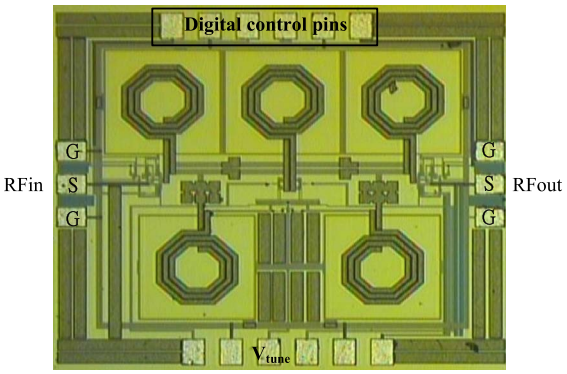

FIGURE 9. Die photograph of the reflection-type phase shifter.

The chip was measured by directly on-wafer probing the pads utilizing the two-port network analyzer. The control voltage, V_{tune}, of the reflective loads and the 6-bit digital switching of the attenuator/RF-tuner were applied via the DC probe pins to adjust the phase shift and transmission amplitude, respectively.

A. MEASURED RTPS PERFORMANCE

Fig. 10 illustrates the full band response of the input reflection and transmission coefficients (S_{11} and S_{21}) at the maximum power gain state where V_{tune} varies from 0 to 1.8 V. It is noted that all the S_{11} can be lower than −10 dB from 3.2 GHz to 3.8 GHz as the reflective loads change. The transmission coefficients versus frequency at 3.5 GHz deviate lower than around 5 dB from the maximum to the minimum values of −8.87 dB and −13.7 dB. The insertion loss comprises the attenuator stage, merged coupler and RF tuner, and reflective loads. The dominant loss contribution is determined by on-chip inductors with parasitic resistors which further degrades the quality factor of inductors. However, a lossy RF path can be compensated by other active devices. In addition, the S_{21} deviations of each voltage states might result from the low loaded quality factor of the reflective C–L–C resonator. For practical exploitation, the deviation of the transmission

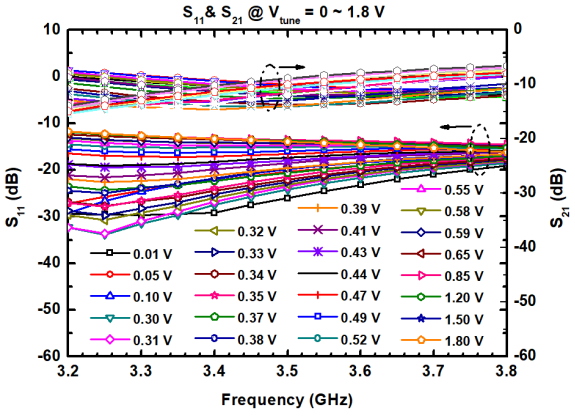

FIGURE 10. Measured input reflection and transmission coefficients versus V_{tune} at the maximum power gain state.

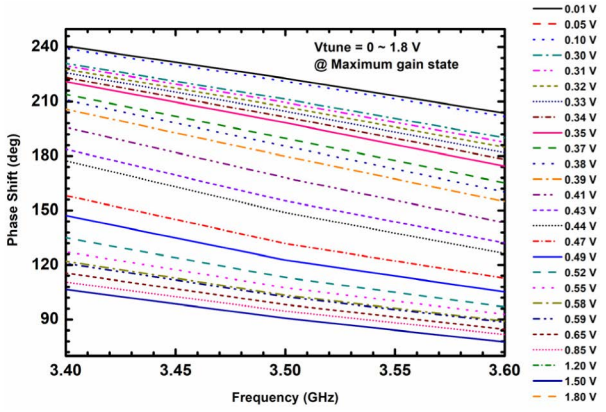

FIGURE 11. Measured relative phase shift versus frequency.

coefficient can be alleviated by a wide power tunning range and the subsequent GA calibration for the phase-array application. Fig. 11 depicts that the measured relative phase shift ranges at 3.4, 3.5, and 3.6 GHz were 133°, 132.7°, and 126.4°, respectively. It is observed that the phase shift range at 3.6 GHz is a bit lower than those of other frequencies. The RTPS bandwidth of around 200 MHz can be used for the beamforming application. From the viewpoint of transmission power adjustment, the measured S_{11} and S_{21} over the operating frequency band with respect to the attenuated control bits at V_{tune} = 0 V are shown in Fig. 12. The transmission power loss is varied by switching the 6-bit MOSFET on/off switch, where the former 4-bit digital control (V_{G1}/V_{G1B} and V_{G2}/V_{G2B}) aims to achieve a power loss range of 8 dB with coarse-tuning steps of 4 dB and the latter is responsible for a 3 dB control range with a fine-tuning resolution of 1 dB by 2-bit binary switching. Thus, the proposed topology of this circuit provides more than 11 dB power control dynamic range with 1 dB resolution. The digital codes of <0,0,1,1,0,0>, <0,1,1,0,0,0>, and <1,1,0,0,0,0> for coarse-tuning attenuation represent the 0, −4, and −8 dB transmission losses, respectively. The corresponding measured phase shift ranges in each coarse-tuning attenuation state are 132.7°, 127.7°, and 129.7° with a phase range deviation of only 5° at the desired frequency of 3.5 GHz. In addition, the reflection coefficients exhibit approximately the same performance of lower than −10 dB as each tuning state. Notably, the small transistor size of the 2-bit attenuation array with only 1 dB step for the merged lumped-element coupler/RF-tuner limits the deterioration of S_{11} and total phase shift as attenuation state varies, which is consistent with the simulation results. Fig. 13 shows the measured maximum relative attenuation error of lower than ± 0.1 dB with 1 dB resolution at RF frequency of 3.5 GHz. The overall dynamic switching achieves linear-in-dB behavior.

Table 1 lists the summarized performance of reported reflection-type phase shifter chip. The state-of-the-art works in [8], [17], [18], [19], [20], [21], [22], and [23] are implemented in millimeter wave frequencies, which occupy small chip areas due to shorter wavelengths. The work in [16]

TABLE 1. Summarized results of reported reflection-type phase shifter.

Ref.	Technology	Frequency (GHz)	Insertion loss (dB)	Return loss (dB)	Phase shift range (deg)	Magnitude control range (dB)	Chia area (mm^2)	No. of varactors
[8]	65 nm CMOS	29	9.5	18	360	0	0.23	4
[16]	180 nm CMOS	2.45	6.8	> 10	120	0	0.72	2
[17]	130nm BiCMOS	62	9.6	10.4	367	0	0.16	4
[18]	28 nm CMOS	44-52	6.2	> 10	90	0	0.08	0[b]
[19]	65 nm CMOS	28	15.5	9.8	180[a]	3	0.17	2
[22]	130 nm CMOS	22.5	10.5	> 10	136	0	0.28	4
[23]	180 nm CMOS	1.9	7.3	23	360	0	2.5	4
[24]	65 nm CMOS	60	7.8	10	130	0	0.041	3
This work	180 nm CMOS	3.5	8.87[c]	13.5	132.7	11	1.25	2

[a]Digital control with a phase resolution of 11.25°
[b]Using a switched capacitor array
[c]Including a two-stage attenuator

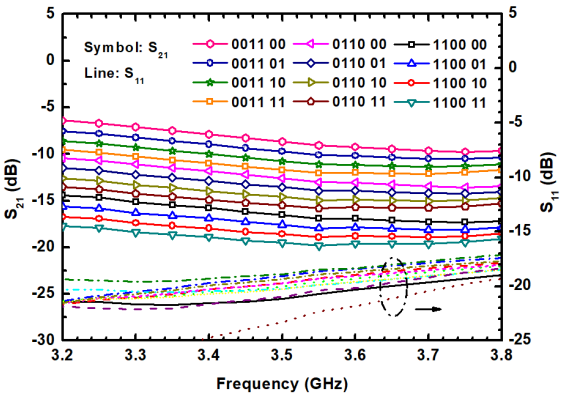

FIGURE 12. Measured S_{21} and S_{11} as a function of the attenuated control bits.

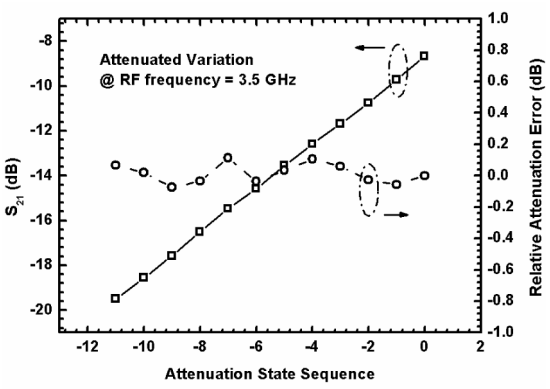

FIGURE 13. Measured attenuation states and relative attenuation error with 1-dB resolution.

also adopts a lump-element coupler with two inductors and only occupies 0.72 mm^2 to realize the reflection-type phase shifter. However, the proposed RF tuner cannot be integrated with the coupler to form a merged topology for simultaneous phase/amplitude control. In addition, although this work only exhibits the phase shift range of around 133°, fewer varactors are used in comparison to other reported ones which has potential to extend the phase range at the expense of higher

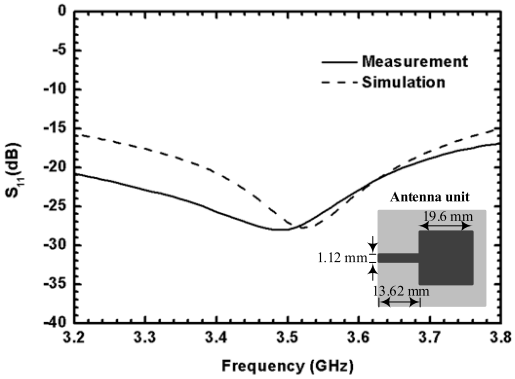

FIGURE 14. Input reflection coefficient of a square patch antenna unit integrated with the merged RTPS/attenuator module.

number of varactors. It is noting that the magnitude control mechanism is also realized in [19] with a tuning range of 3 dB. The approach proposed in this work presents a magnitude control of 11 dB with a fine-tuning resolution of 1 dB.

B. EXAMINATION OF THE 1 × 8 PHASED-ARRAY ANTENNA WITH RTPS

A 1 × 8 phased-array antenna with the merged RTPS/ attenuator for phase and power controls is adopted to investigate the performance of the beamforming characteristics. Accordingly, a conventional square microstrip patch antenna integrated with this merged circuit is fabricated by a standard FR-4 printed circuit board with a board thickness of 1.6 mm. The RTPS with input/output bonding wires connects to the input port and the subsequent antenna unit. The integrated board adopts an SMA connector for measurement. Fig. 14 depicts the consistent simulated and measured reflection coefficients of the testing board. The full band frequency response of S_{11} is lower than −10 dB at a maximum power state. In addition, the integrated prototype is regarded as a sub-array unit for planning a 1 × 8 high-gain phased-array antenna in parallel with proper antenna design parameters and fixed distance of around half wavelength at 3.5 GHz between

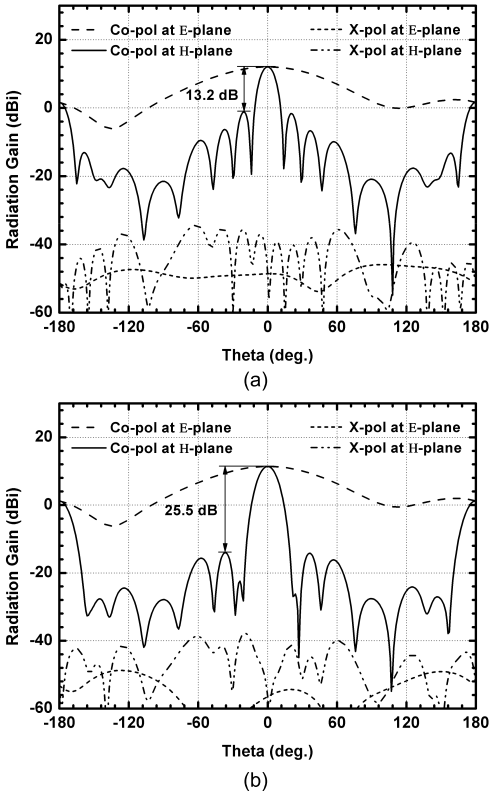

FIGURE 15. Radiation pattern of 1 × 8 high-gain phased-array antenna with (a) equal feeding energy and (b) feeding ratio of 1:2:5:8:8:5:2:1.

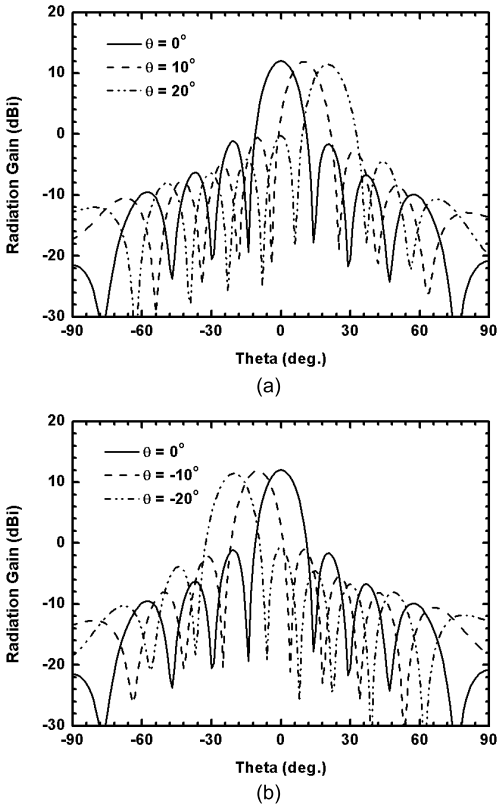

FIGURE 16. Beam deviation pattern of 1 × 8 phased-array antenna with (a) positive and (b) negative beam deviations.

each unit. However, considering the difficulties in controlling a substantial number of digital/analog voltage control pins for the beamforming application, the precision of the DC power supply instruments, and the lack of an anechoic chamber in the measurement environment, the simulated radiation behavior is utilized to evaluate the performance of the phased-array antenna pattern. Fig. 15(a) illustrates the radiation pattern of a 1 × 8 phased-array antenna with equal feeding energy, which exhibits the maximum antenna gain of 12.05 dBi with half power beam widths of 13° along the H-plane. The first side-lobe of radiation gain is suppressed greater than 13 dB. However, considering the first side-lobe beam still larger than −1 dBi, the proposed merged RTPS/attenuator module provides a phase/amplitude beamforming circuit to further suppress sidelobes. Therefore, the distributions of equal phase and feeding energy ratio of 1:2:5:8:8:5:2:1 at each input port are applied to further eliminate the unwanted sidelobes. It is observed that the first side-lobe lower than −20 dBi is achieved, as depicted in Fig. 15(b). The maximum side-lobe energy has moved to the 2nd sidelobe beam at $\theta = \pm 36°$, which obtains a suppression value of 25.5 dB compared with the main beam. The beamforming technique with unequal feeding energy ratio based on the merged RTPS/attenuator exhibits approximately 12.2 dB improvement from the same injecting power. The second side-lobe with a wider radiation angle also reduces the influence of the main beam. These comparisons demonstrate that the proposed RTPS with power control mechanism greatly improves the radiation efficiency for the phased-array antenna. Additionally, a fixed phase shift between adjacent sub-array units for 1-D beam scan is performed to achieve beam deviation and then investigate beamforming characteristic of the phased-array antenna. Fig. 16 depicts the radiation pattern with beam offset angles (θ) from −20° to 20° in 10° step. The corresponding gains of each deviated main beam are 11.45, 11.91, 12.05, 12.05, 11.91, 11.45 dBi, respectively.

V. CONCLUSION

This paper proposes a way of achieving phase/amplitude tuning on the same RTPS chip by integrating the quadrature coupler and RF tuner. The RF tuner provides an RF reduction path that is compatible with the high/low pass lumped-element coupler and maintains the performance of the RTPS operation. Meanwhile, the coarse- and fine- tunings of the attenuation are incorporated to form a linear-in-dB power control for a phased-array beamforming. The simulated and experimental results demonstrate the viability of this merged couple/RF-tuner concept by examining the properties of the S-parameters and phased-array radiation patterns.

ACKNOWLEDGMENT

The authors would like to thank the editor and anonymous reviewers for their valuable comments, time, and suggestions for improving the quality of the paper.

REFERENCES

[1] M. Gidlund, T. Lennvall, and J. Akerberg, "Will 5G become yet another wireless technology for industrial automation?" in *Proc. IEEE Int. Conf. Ind. Technol. (ICIT)*, Mar. 2017, pp. 1319–1324.
[2] N. Al-Falahy and O. Y. Alani, "Technologies for 5G networks: Challenges and opportunities," *IT Prof.*, vol. 19, no. 1, pp. 12–20, Jan. 2017.
[3] X. Cheng, N. Lou, and S. Li, "Spatially sparse beamforming training for millimeter wave MIMO systems," *IEEE Trans. Wireless Commun.*, vol. 16, no. 5, pp. 3385–3400, May 2017.
[4] J. M. Johnson and V. Rahmat-Samii, "Genetic algorithms in engineering electromagnetics," *IEEE Antennas Propag. Mag.*, vol. 39, no. 4, pp. 7–21, Aug. 1997.
[5] G. Brenna, D. Tschopp, J. Rogin, I. Kouchev, and Q. Huang, "A 2-GHz carrier leakage calibrated direct-conversion WCDMA transmitter in 0.13-μm CMOS," *IEEE J. Solid-State Circuits*, vol. 39, no. 8, pp. 1253–1262, Aug. 2004.
[6] H.-H. Kuo, Y.-H. Li, and Y.-H. Pang, "A 0.13 μm CMOS transmitter with 72-dB RF gain control for mobile WiMAX/WiBro applications," in *Proc. IEEE Radio Freq. Integr. Circuits Symp.*, Jun. 2008, pp. 105–108.
[7] R. Bourtoutian and P. Ferrari, "Tapered distributed analogue tunable phase shifter with low insertion and return loss," *Electron. Lett.*, vol. 41, no. 15, pp. 852–854, Jul. 2005.
[8] A. Basaligheh, P. Saffari, S. R. Boroujeni, I. Filanovsky, and K. Moez, "A 28–30 GHz CMOS reflection-type phase shifter with full 360° phase shift range," *IEEE Trans. Circuits Syst. II, Exp. Briefs*, vol. 67, no. 11, pp. 2452–2456, Nov. 2020.
[9] P. Anand, S. Sharma, D. Sood, and C. C. Tripathi, "Design of compact reconfigurable switched line microstrip phase shifters for phased array antenna," *Emerg. Tech. Trends Electron., Commun. Netw.*, vol. 19, pp. 1–3, Dec. 2012.
[10] F. Golcuk, T. Kanar, and G. M. Rebeiz, "A 90–100-GHz 4×4 SiGe BiCMOS polarimetric transmit/receive phased array with simultaneous receive-beams capabilities," *IEEE Trans. Microw. Theory Techn.*, vol. 61, no. 8, pp. 3099–3114, Aug. 2013.
[11] A. Singh and M. K. Mandal, "Electronically tunable reflection type phase shifters," *IEEE Trans. Circuits Syst. II, Exp. Briefs*, vol. 67, no. 3, pp. 425–429, Mar. 2020.
[12] M. Askari, H. Kaabi, and Y. Kavian, "A 24 GHz reflective-type phase shifter with constant loss in 0.18 μm CMOS technology," *Int. J. Electron. Commun.*, vol. 69, no. 8, pp. 1134–1142, Apr. 2015.
[13] R. Garg and A. S. Natarajan, "A 28-GHz low-power phased-array receiver front-end with 360° RTPS phase shift range," *IEEE Trans. Microw. Theory Techn.*, vol. 65, no. 11, pp. 4703–4714, Nov. 2017.
[14] C. S. Lin, S. F. Chang, and W. C. Hsiao, "A full 360° RTPS with constant insertion loss," *IEEE Microw. Wireless Compon. Lett.*, vol. 18, no. 2, pp. 106–108, Feb. 2008.
[15] H. L. Lee, S.-M. Moon, M.-Q. Lee, and J.-W. Yu, "Design of compact broadband phase shifter with constant loss variation," *Microw. Opt. Technol. Lett.*, vol. 56, no. 2, pp. 394–400, Feb. 2014.
[16] J. C. Wu, T. Y. Chin, S. F. Chang, and C. C. Chang, "2.45-GHz CMOS reflection-type phase-shifter MMICs with minimal loss variation over quadrants of phase-shift range," *IEEE Trans. Microw. Theory Techn.*, vol. 56, no. 10, pp. 2180–2189, Oct. 2008.
[17] T.-W. Li and H. Wang, "A millimeter-wave fully integrated passive reflection-type phase shifter with transformer-based multi-resonance loads for 360° phase shifting," *IEEE Trans. Circuits Syst. I, Reg. Papers*, vol. 65, no. 4, pp. 1406–1419, Apr. 2018.
[18] S. Dong, Z. Chen, H. Jia, W. Deng, and B. Chi, "A 44–52 GHz reflection-type phase shifter with 1.4° phase resolution in 28 nm CMOS process," in *Proc. IEEE Int. Conf. Integr. Circuits, Technol. Appl. (ICTA)*, Nov. 2020, pp. 15–16.
[19] M. Kadam, A. Kumar, and S. Aniruddhan, "A 28 GHz reflective-type transmission-line-based phase shifter," *IEEE Trans. Circuits Syst. I, Reg. Papers*, vol. 67, no. 12, pp. 4641–4650, Dec. 2020.
[20] F. Burdin, Z. Iskandar, F. Podevin, and P. Ferrari, "Design of compact reflection-type phase shifters with high figure-of-merit," *IEEE Trans. Microw. Theory Techn.*, vol. 63, no. 6, pp. 1883–1893, Jun. 2015.
[21] J. A. Hou and Y. H. Wang, "A compact quadrature hybrid based on high-pass and low-pass lumped elements," *IEEE Microw. Wireless Compon. Lett.*, vol. 17, no. 8, pp. 595–597, Aug. 2007.
[22] A. B. Nguyen and J.-W. Lee, "A K-band CMOS phase shifter MMIC based on a tunable composite metamaterial," *IEEE Microw. Wireless Compon. Lett.*, vol. 21, no. 6, pp. 311–313, Jun. 2011.
[23] H. Zarei, C. T. Charles, and D. J. Allstot, "Reflective-type phase shifters for multiple-antenna transceivers," *IEEE Trans. Circuits Syst. I, Reg. Papers*, vol. 54, no. 8, pp. 1647–1656, Aug. 2007.
[24] S. Shamsadini, I. M. Filanovsky, P. Mousavi, and K. Moez, "A 60-GHz transmission line phase shifter using varactors and tunable inductors in 65-nm CMOS technology," *IEEE Trans. Very Large Scale Integr. (VLSI) Syst.*, vol. 26, no. 10, pp. 2073–2084, Oct. 2018.

CHIA-HUNG CHANG (Member, IEEE) received the B.S. degree in electrical engineering from Yuan Ze University, Taoyuan, Taiwan, in 2004, and the M.S. and Ph.D. degrees in communication engineering from the National Chiao Tung University, Hsinchu, Taiwan, in 2006 and 2012, respectively. From 2011 to 2013, he was a Research Assistant with the National Applied Research Laboratory, Hsinchu. He is currently an Associate Professor with the Department of Electrical Engineering, National Yunlin University of Science and Technology. His current research interest includes developing RF/microwave integrated circuits.

JO-YU CHEN is currently pursuing the M.S. degree in electrical engineering with the National Yunlin University of Science and Technology, Taiwan. His current research interests include the design of phased array of antennas and microwave couplers for the applications of the fifth generation of mobile communications.

CHE-TIEN SHEN is currently pursuing the B.S. degree in electrical engineering with the National Yunlin University of Science and Technology, Taiwan. His current research interests include the patch antenna design for the applications of the radar and fifth generation of mobile communications.

MENG-JU TSAI is currently pursuing the M.S. degree in electrical engineering with the National Yunlin University of Science and Technology, Taiwan. His current research interest includes the design of CMOS RF/microwave integrated circuits for the applications of the fifth generation of mobile communications.

TSE-SHENG TAI received the B.S. degree in electrical engineering from Feng Chia University, Taichung, Taiwan, in 2020. He plan to pursue the M.S. degree. His current research interests include the design of phase shifter and RF/microwave front-end integrated circuit for mobile communications.